HHS Public Access

Author manuscript

J Org Chem. Author manuscript; available in PMC 2016 September 04.

Published in final edited form as:

J Org Chem. 2015 September 4; 80(17): 8713–8719. doi:10.1021/acs.joc.5b01486.

Application of 3D NMR for Structure Determination of Peptide Natural Products

Fan Zhang[†], **Navid Adnani**[†], **Emmanuel Vazquez-Rivera**[‡], **Doug R. Braun**[†], **Marco Tonelli**[§], **David R. Andes**[‖], and **Tim S. Bugni**[*,†]

[†]Pharmaceutical Sciences Division, University of Wisconsin–Madison, Madison, Wisconsin 53705, United States

[‡]Molecular & Environmental Toxicology Center, University of Wisconsin–Madison, Madison, Wisconsin 53705, United States

[§]National Magnetic Resonance Facility at Madison, University of Wisconsin–Madison, Madison, Wisconsin 53706, United States

[‖]Department of Medicine, University of Wisconsin–Madison, Madison, Wisconsin 53705, United States

Abstract

Despite the advances in NMR, structure determination is often slow and constitutes a bottleneck in natural products discovery. Removal of this bottleneck would greatly improve the throughput for antibiotic discovery as well as other therapeutic areas. Overall, faster structure methods for structure determination will serve the natural products community in a broad manner. This report describes the first application of 3D NMR for elucidation of two microbially produced peptide natural products with novel structures. The methods are cost-effective and greatly improve the confidence in a proposed structure.

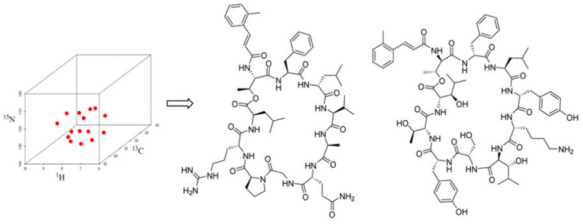

INTRODUCTION

Drug resistant infectious diseases, in particular Gram-negative infections, continue to threaten global health as well as contemporary medical practices.[1] For example, as

[*]**Corresponding Author** Tel.: 1-608-263-2519. tim.bugni@wisc.edu..

Supporting Information

The Supporting Information is available free of charge on the ACS Publications website at DOI: 10.1021/acs.joc.5b01486. NMR data, MS data, and Marfey's analysis for compounds **1** and **2**. (PDF)

The authors declare no competing financial interest.

pathogens become increasingly resistant, semiroutine procedures such as organ transplants and joint replacements will become increasingly dangerous. Combined with the emergence of pan-resistant pathogens, new antibiotics are sorely needed. Although natural products have provided the antibiotic basis upon which many medical practices were built, discovering novel antibiotics has become more challenging. Nonetheless, advances in sequencing and genomics has not only indicated that there is more potential than previously thought, but also have provided tools for nearly routine analyses of the genetic potential of bacteria to produce small molecules, many of which would have antibiotic potential.[2,3] In parallel, analytical strategies that take advantage of increasing sensitivity of mass spectrometers as well as the speed and resolving power of UPLC systems have enabled rapid identification of novel antibiotics.[3–12] Combining these new tools with the bacterial diversity found in underexplored ecological niches such as insect symbionts,[13] thermal vents,[14] caves,[15] coal mines,[16] and marine ecosystems[17] has demonstrated great promise for discovering the next generation of antibiotic therapies.

To address the challenges of resistant infectious disease, the potential of these genetic and analytical methods must be fully realized. Our lab has focused on LCMS-based metabolomics as a discovery platform to discover novel natural products from marine invertebrate-associated bacteria. This has led to a high discovery rate of novel natural products.[8–11] As these methods pave the way for rapid discovery, structure determination becomes a limiting factor for providing valuable lead structures. Therefore, we have developed methods such as isotopic labeling followed by ^{13}C–^{13}C gCOSY[11,18,19] for rapid assembly of carbon backbones in polyketides and ^{13}C–^{15}N NMR[11] to assist with thiazolines and other heterocyclic systems. While our previous studies demonstrated a high level of ^{13}C enrichment could be achieved for molecules of acetate origin, questions remained surrounding isotopically labeling peptides. For example, typical growth media used were rich in natural abundance precursors such as amino acids from sources like yeast extract and peptone. On the other hand, if uniform labeling could be achieved for both ^{13}C and ^{15}N, structure determination of peptide-based natural products could be achieved using biomolecular NMR strategies such as 3D NMR techniques. These approaches would also provide a gateway to automated backbone assignment of structures containing typical amino acids. Therefore, we evaluated isotopic labeling in a medium that contained typical quantities of nonenriched components. To demonstrate proof of concept for both isotopic labeling and 3D NMR strategies, we tested the methods using two novel antibiotic peptides, one of which was prioritized as part of an antibiotic drug discovery program. In particular, peptide **2** showed broad spectrum activity including against Gram-negative pathogens. Although peptide **2** did not show high potency, the difference between the MIC (22.7 μM) and MBC (45.5 μM) was small indicating potential for Gram-negative infections. The overall goal of this study was to provide a basis for reducing structure determination times from months to hours or days.

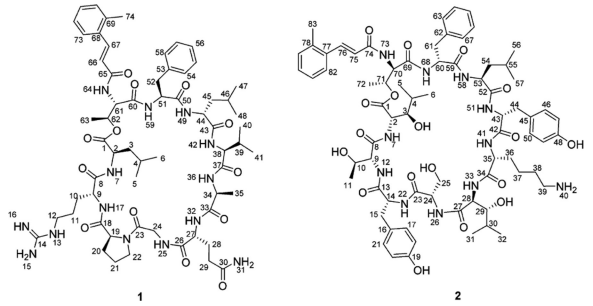

RESULTS AND DISCUSSION

Uniform Labeling Peptides with ^{13}C and ^{15}N

Our previous studies showed that fermentation of actinobacteria upon addition of uniformly ^{13}C-labeled glucose and subsequent purification yielded ^{13}C-labeled natural products.[19] However, peptides could be more challenging since in most cases U–^{13}C glucose was utilized for ^{13}C enrichment in natural products which have been biosynthesized via a polyketide pathway.[11,20] For the ^{15}N incorporation, $^{15}NH_4Cl$ was evaluated as the nitrogen source. As mentioned, a potential issue was ^{15}N incorporation with peptides in rich media. To evaluate the ^{13}C and ^{15}N incorporation, a marine invertebrate-derived *Streptomyces* sp. (strain WMMB 705) that produced two novel peptides that we named eudistamides A (**1**) and B (**2**) was grown in multiple media and extracts were analyzed by LC–MS data (Supporting Information). Although the medium containing $^{15}NH_4Cl$ as the only nitrogen source (M3, Supporting Information) yielded the highest ^{15}N abundance of the peptides, taking into consideration the various factors such as the price of the medium, the yield, and the ^{13}C and ^{15}N abundance, the labeled medium containing peptone and yeast extract (20 g soluble starch, 10 g [U–^{13}C] glucose, 2.5 g peptone, 2.5 g yeast extract, 5 g $^{15}NH_4Cl$, 5 g $CaCO_3$/L of artificial seawater) was used for producing ^{13}C- and ^{15}N-labeled peptides.

Strategies and Experiments for the Resonance Assignment of Uniformly ^{13}C, ^{15}N-Labeled Peptides

Backbone Assignment Strategy—A typical triple resonance 3D NMR spectrum observes correlations of three resonances, a proton, a carbon, and a nitrogen. Many 3D NMR experiments have been designed for assigning the backbone of $^{15}N/^{13}C$ isotopically labeled protein, such as HNCO,[21] NH(CA)CO,[22] HNCA,[21] CBCANH,[23] CBCA(CO)NH,[24] HN(CO)CA,[25] HCACO,[21] HCA(CO)N,[21] H(CCO)NH,[26] C(CO)NH,[26] and HBHA(CBCACO)NH.[27] Ideally, standard triple resonance backbone assignment of a peptide has relied on a combination of the CBCANH, CBCA(CO)NH, and NHCO spectra (Figure 1a–c). The general idea was that the CBCANH correlated each NH group with the C_α and C_β chemical shifts of its own residue (strongly) and of the preceding residue (weakly), whereas the CBCA(CO)NH only correlates the NH group to the preceding C_α and C_β chemical shifts. The NHCO experiment provides the connectives between each NH group with the carbonyl carbon of the preceding residue, thus establishing the backbone assignment. In our experience, the quality of the CBCANH and CBCA(CO)NH spectra was sometimes not sufficient in terms of S/N. The C_α or C_β resonances were, for example, not

visible above the noise level. In this case, the combination of HNCA and HN(CO)CA experiments (Figure 1e–f) which were more sensitive provided the same information as the CBCANH and CBCA(CO)NH spectra, except without the C_β resonances. The HN(CA)CO experiment (Figure 1d) was powerful for linking each NH group with the carbonyl carbon of the same residue, particularly helpful to the assignment of depsipeptides. A depsipeptide is a peptide in which one or more of its –C(O)NHR groups are replaced by the corresponding ester, –C(O)OR. Taking eudistamides A (**1**) and B (**2**) for example, no correlation for C-1 could be seen in NHCO spectrum, whereas HN(CA)CO experiment could correlate NH-7 with the carbonyl carbon of the ester (C-1). Therefore, our backbone assignment strategy used three 3D NMR experiments, HNCO, CBCANH, and CBCA(CO)NH, to establish the connectivity of the backbone as the first step. The other 3D NMR experiments, NHCA, HN(CO)CA, NH(CA)CO, were utilized to make further confirmation regarding to some complicated cases, such as overlapping carbonyl carbon signals and any crosspeak that was very weak or missing in either CBCANH or CBCA(CO)NH spectrum. We were thereby able to make unambiguous backbone assignment of the eudistamides A and B and provided a general strategy for non-Pro containing peptide natural products. However, due to the absence of an amide proton in proline, these 3D NMR experiments cannot be used to sequentially connect proline residue to the preceding residue. The CDCA(NCO)CAHA (Figure 1h) was designed for the sequential assignment of proline residues,[28] and the other option is to rely on the observation of NOEs to neighboring residues.

Side Chain Assignment Strategy—Depending on the structure, side chains can be assigned using TOCSY and HSQC. However, the most useful NMR experiment for side chain assignment is an HCCH-TOCSY spectrum (Figure 1g).[29] The general principle behind using the HCCH-TOCSY spectrum is as follows: Using the known C_α and C_β chemical shifts from the backbone assignment, the side chain chemical shifts would be assigned by viewing 2D slices at each carbon shift, typically at the C_α and C_β chemical shifts. Each "slice" contains resonances for the protons attached to carbons in that ^{13}C–^{13}C spin system. The HCCH-TOCSY experiment combined with ^{13}C chemical shift ranges of the common amino acids provides a very powerful means for the assignment of the aliphatic side chain. Some of the proteinogenic amino acids, such as alanine, serine, threonine and glycine, were easily identified since alanine, serine, and threonine's C_β chemical shifts were unique compared to those of the other amino acids and glycine has no C_β. Valine, isoleucine, and proline could also be easily identified because they have lower than normal C_α chemical shifts. For the aromatic side chain assignment, such as tyrosine, phenylalanine, tryptophan, and histidine, additional 2D NMR data are needed to complete the whole side chain assignment.

Structure Elucidation of Eudistamides A (1) and B (2)

Eudistamide A (**1**) was obtained as a white powder with a molecular formula of $C_{61}H_{90}N_{14}O_{13}$, determined by HRESIMS. Interpretation of HCCH-TOCSY data (Table S1; Supporting Information) of the ^{13}C- and ^{15}N-doubly labeled **1** established the amino acid residues leucine (Leu; 2×), arginine (Arg), proline (Pro), glycine (Gly), glutamine (Gln), alanine (Ala), valine (Val), and phenylalanine (Phe), which were further confirmed by natural abundance experiments, ^1H–^1H COSY, HSQC and HMBC data (Table S3;

Supporting Information). The Pro residue was assigned as *cis* based on the ^{13}C NMR chemical shifts of the β- and γ-carbon atoms ($\Delta\delta_{\beta\gamma}$). $\Delta\delta_{\beta\gamma}$ for *trans*-Pro is regularly less than 5 ppm, while $\Delta\delta_{\beta\gamma}$ for *cis*-Pro is regularly between 5 and 10 ppm.[30] $\Delta\delta_{\beta\gamma}$ for the proline residue in **1** was 5.8 ppm, supporting the assignment as *cis*. The 3-(2-methylphenyl)acrylic acid (Me-acyl) moiety was established by HMBC, whereas geometry of the double bond (C_{66} and C_{67}) was assigned as *E* on the basis of large coupling constant (15.5 Hz) through the double bond.

The connectivity of the partial structures Thr-Phe-Leu_2-Val-Ala-Gln-Gly and Pro-Arg-Leu_1 was established by using 3D NMR data which were discussed for the backbone assignment (CBCANH, CBCACONH, NHCO, HNCA, NH(CO)CA, NH(CA)CO; Table S1; Supporting Information) of the ^{13}C- and ^{15}N-doubly labeled **1**. The HMBC correlation from H-62 to C-1 and the ROESY correlation between H_3-63 and H-2 connected Leu_1 to Thr via an ester on the basis of the chemical shift of C-62 (δc 68.5). Moreover, for the uncommon amino acid residue, the HMBC correlations from H-66 and H-67 to C-65 supported the linkage of Me-acyl moiety to Thr. The ROESY correlations between H-24a and H_2-22 secure the ring closure by connecting the Gly unit to Pro, which satisfied the 24 degrees of unsaturation deduced from the molecular formula.

The advanced Marfey's method[31] was applied to assign the absolute configurations of the amino acid residues from acid hydrolysis of **1**. The 1-fluoro-2,4-dinitrophenyl-5-leucine-amide (FDLA) derivatives of the hydrolysate of **1** and authentic D- and L-amino acids were subjected to LC–MS analysis. The absolute configuration of all amino acids was established by comparison of their HPLC retention time and molecular weights with those of corresponding authentic D- and L-standards. Upon analysis, the amino acid residues Arg, Pro, Ala, Val, *allo*-Thr, and Phe were determined to have the L-configuration, whereas the Gln and Leu were deduced to have the D-configuration (Table S5; Supporting Information).

Eudistamide B (**2**) was isolated a white amorphous powder with a molecular formula of $C_{72}H_{99}N_{11}O_{18}$ as determined by HRESIMS. A detailed analysis of HCCH-TOCSY (Table S2; Supporting Information) of the ^{13}C- and ^{15}N-doubly labeled **2** indicated an amino acid content as follows: Thr (×2), Tyr (×2), Ser, Lys, 3-OH-Leu (×2), Leu, and Phe. CBCANH, CBCA(CO)NH NHCO, HNCA, NH(CO)CA, and NH(CA)-CO spectra (Table S2; Supporting Information) revealed the amino acids sequence as 3-OH-Leu_1-Thr_1-Tyr_1-Ser-3-OH-Leu_2-Lys-Tyr_2-Leu-Phe-Thr_2, which was further confirmed by ESIMS/MS fragmentation analysis (Figure S22; Supporting Information). The linkage of Me-acyl moiety to Thr_2 was supported by the HMBC correlation from H-76 to C-74. The ROESY correlation between H_3-72 and H-2 and consideration of unsaturation deduced from the molecular formula connected 3-OH-Leu_1 to Thr_2 via an ester on the basis of the chemical shift of C-71 (δc 68.5).

The absolute configurations of the amino acids were determined using acid hydrolysis followed by the advanced Marfey's method. The chromatographic comparison between Marfey's derivatives of the hydrolysate of **2** and appropriate amino acid standards assigned the L-configurations for Ser and Leu and D-configurations for Lys, Phe, allo-Thr, and Tyr (Table S4; Supporting Information). The (2*R*, 3*S*) and (2*R*, 3*R*)-3-hydroxyleucine were

synthesized following Bonnard's procedure[32] and derivatized with L- and L/D-FDLA respectively. Since enantiomers would exhibit identical retention behavior under nonchiral HPLC conditions, the (2*R*, 3*S*)-D-FDLA derivative showed the same retention time as (2*S*, 3*R*)-L-FDLA, whereas the (2*R*, 3*R*)-D-FDLA derivative showed the same retention time as (2*S*, 3*S*)-L-FDLA. By comparing the above the four retention times of the 3-OH-Leu standards with the L-FDLA derivatives of the hydrolysate of **2**, both the 3-OH-Leu in **2** were assigned as 2*S*, 3*R* (Table S6; Supporting Information). The 2*S*, 3*R* configuration of the two 3-hydroxyleucines in **2** were also confirmed by *J*-based analysis and NOESY data. The large coupling constants observed from DQF-COSY in MeOD between H-2 and H-3 (11.5 Hz), and between H-28 and H-29 (11.0 Hz) established their anti-relationship. The ROESY correlation between H-4 and NH-7, as well as the ROESY correlation between H-30 and NH-33, established the rotamer (A4) in Figure 2.

Compounds **1** and **2** were tested for antibacterial activity against *Pseudomonas aeruginosa*, Methicillin-resistant *Staphylococcus aureus* (MRSA), *Escherichia coli*, and *Bacillus subtilis*. Compound **2** showed antibacterial activity against MRSA, *E. coli* and *B. subtilis*, with the MIC values of 22.7, 22.7, and 2.8 μM, respectively, while compound **1** did not show any detectable antibacterial activities at 52.2 μM. Compound **2** was also tested using a murine thigh model infected with either *E. coli* ATCC 25922 or *S. aureus* ATCC 25923 (Figure 3). Over the 16-fold intraperitoneal dose range, no toxicity associated with compound administration was observed (Figure 3a,c). Conversely, intravenous dose levels above 8 mg/kg resulted in animal death (Figure 3b,d). Modest, but broad spectrum (both Gram-positive and Gram-negative bacteria) efficacy was observed with two highest tolerated dose levels given by both administration routes. Compared to untreated control animals, compound **2** reduced the organism burden in the thighs of immunocompromised mice by more than 0.5 $\log_{10}$ cfu/thigh.

Although the cyclopetides and cyclodepsipeptides have been encountered frequently as bacterial secondary metabolites, eudistamides A (**1**) and B (**2**) differ markedly from the known peptides by virtue of the presence of a unique 3-(2-methylphenyl)acrylic acid moiety, which has not been previous reported in a peptide. Only some analogues of 3-(2-methylphenyl)acrylic acid residue were rarely descried in peptides, such as WS9326s,[33] pepticinnamins,[34] and mohangamides[35] incorporating a 2-pentenyl cinnamic acid moiety, skyllamycins A and B[36,37] incorporating a 2-propenyl]-cinnamic acid moiety, and corprisamides A and B bearing 2-heptatrienyl cinnamic acid moiety.[38] Moreover, another remarkable feature of compound **2** is the high content of the β-hydroxy-α-amino acids, including genetically coded proteinogenic amino acids Ser and Thr, and nonstandard amino residue 3-OH-Leu. Members of the β-hydroxy-α-amino acid class occur as constituents of many important antibiotics, such as vancomycin[39] and lysobacin.[40] Furthermore, compounds **1** and **2** could be produced in sufficient quantities by scale-up microbial fermentation, which would greatly facilitate follow-up mechanistic and preclinical studies.

CONCLUSION

The introduction of 3D NMR has dramatically improved the speed and reliability of the protein assignment process.[22,41] However, we expanded the scope of 3D NMR experiments

from protein applications to a strategy that is universally applicable for labeled peptides. We have demonstrated a rapid and efficient structure elucidation protocol for complex peptides containing typical amino acids. The protocol we propose consists of a typical set of 3D NMR experiments for backbone and side chain assignment of uniformly labeled peptides with ^{13}C and ^{15}N. While 3D NMR experiments may not be optimal for natural product peptides, this proof of concept provides a basis for using triple resonance strategies for rapidly establishing the backbone of peptide natural products. Development of specific NMR experiments would be advantageous. The triple resonance experiments used in this study were highly complementary to more traditional methods such as HMBC and ROESY. This report describes the first application of 3D NMR to two microbially produced peptide natural products with novel structures. The methods are cost-effective and greatly improve the confidence in a proposed structure.

EXPERIMENTAL SECTION

General Experimental Procedures

Optical rotations were measured on a Polarimeter. UV spectra were recorded on a UV–vis Spectrophotometer. IR spectra were measured with a FT–IR Spectrophotometer. 1D and 2D NMR spectra were obtained in DMSO with a NMR spectrometer equipped with a $^{13}C/^{15}N\{^{1}H\}$ cryoprobe. 3D NMR spectra were obtained in DMSO with a NMR spectrometer with a ($^{1}H\{^{13}C,^{15}N\}$) cold probe. HRMS data were acquired with a QTOF mass spectrometer (Ionization method: Spray Voltage (+) 4000; Spray Voltage (−) 3700; Capillary temperature 320; full MS scan 200–2000). MSMS data were acquired with a hybrid quadrupole-Orbitrap mass spectrometer. RP HPLC was performed using a HPLC system and a Phenomenex Luna C_{18} column (250 × 10 mm, 5 μm), as well as a preparative HPLC and Phenomenex Gemini C_{18} column (250 × 30 mm, 5 μm). The Advanced Marfey's method utilized a HPLC coupled with a mass spectrometer.

Biological Material

Ascidian specimens were collected in September 2011 from the Florida Keys (24°33.416′, 81°21.611′). Identification was confirmed by Shirley Parker-Nance. A voucher specimen for *Eudistoma olivaceum* (Van Name, 1902)[42] is housed at the University of Wisconsin—Madison. For cultivation, a sample of ascidian (1 cm^3) was rinsed with sterile seawater and macerated using a sterile pestle in a microcentrifuge tube, and dilutions were made in sterile seawater, with vortexing between steps to separate bacteria from heavier tissues. Dilutions were separately plated on three media: ISP2 supplemented with artificial seawater,[43] R2A,[44] and M4.[45] Each medium was supplemented with 50 μg/mL cycloheximide and 25 μg/mL nalidixic acid. Plates were incubated at 28 °C for at least 28 days, and strain WMMB 705 was purified from an ISP2 isolation plate.

Sequencing

Genomic DNA was extracted using the UltraClean Microbial DNA Isolation kit (Mo Bio Laboratories, Inc.). 16S rDNA genes were amplified using 100–200 ng genomic DNA template with the primers 8–27F (5′ to 3′ GAGTTTGATCCTGGCTCAG) and 1492R (5′ to 3′ GGTTACCTTGTTACGACTT). The following PCR conditions were used: 94 °C for 5

min, followed by 30 cycles of 94 °C for 30 s, 55 °C for 1 min, 72 °C for 1.5 min, with a final step of 72 °C for 5 min. The PCR bands were excised from the gel and purified using the QIAquick Gel Extraction kit (QIAGEN). One microliter of purified product was sequenced. Sequencing reactions were performed by the UW Biotechnology Center and reactions were sequenced with an ABI 3730xl DNA Analyzer. WMMB 705 were identified as *Streptomyces* sp. by 16S sequencing, and demonstrated 99% sequence similarity to *Streptomyces* sp. FXJ6.141 (accession number GU 339421).

Fermentation, Extraction, and Isolation

Two 10 mL of seed cultures (25 × 150 mm tubes) in medium ASW-A (20 g soluble starch, 10 g glucose, 5 g peptone, 5 g yeast extract, 5 g $CaCO_3$ per liter of artificial seawater) were inoculated with strain WMMB 705 and shaken (200 rpm, 28 °C) for 4 days. Two-liter flasks (2 × 500 mL) containing ASW-A medium with Diaion HP20 (7% by weight) were inoculated with 8 mL from the culture tube and shaken at 200 rpm and 28 °C for 7 days. Filtered HP20 was washed with water and extracted with acetone. The acetone extract was chromatographed on Diaion HP20ss, eluting sequentially with methanol/water (10:90 and 95:5). The 95% methanol eluate was evaporated to dryness to afford a yellow oil (460 mg), and then it was subjected to RP HPLC (30%/70% to 60%/40% ACN/H_2O with H_2O containing 0.1% acetic acid over 30 min, 25 mL/min, followed by 90/10% to 100% of the same solvents for 3 min, 25 mL/min, and a hold at 100%/0% of the same solvents) using a Phenomenex Gemini C_{18} column (250 × 30 mm, 5 μm), yielding a fraction containing **1** (50 mg, t_R 11.5 min), and compound **2** (21 mg, t_R 12.5 min). The fraction containing **1** was further subjected to RP HPLC (55–65% MeOH–H_2O with H_2O containing 0.1% acetic acid over 25 min, 4.0 mg/mL) using a Phenomenex Luna C_{18} column (250 × 10 mm, 5 μm), yielding **1** (22 mg, t_R 19 min). For ^{13}C and ^{15}N incorporation, the same procedure was used (1 × 250 mL) with labeled medium ASW-A (20 g soluble starch, 10 g U^{13}C-glucose, 2.5 g peptone, 2.5 g yeast extract, 5 g $^{15}NH_4Cl$, 5 g $CaCO_3$ per liter of artificial seawater).

Antibacterial Assay

Eudistamides A (**1**) and B (**2**) were tested for antibacterial activity against MRSA (ATCC #33591), *E. coli* (ATCC #25922), *B. subtilis*, and *P. aeruginosa* (ATCC #27853), and MICs were determined using a dilution antimicrobial susceptibility test for aerobic bacteria.[46] Eudistamides A (**1**) and B (**2**) were dissolved in DMSO, serially diluted to 10 concentrations (0.125–64 μg/mL), and tested in a 96-well plate. Vancomycin was used as a control and exhibited an MIC of 0.69 μmol against MRSA and 0.69 μmol against *B. Subtilis*. Gentamicin was used as a control and exhibited an MIC of 8.4 μmol against *E. coli* and 8.4 μmol against *P. aeruginosa*. Peptides **1** and **2** were tested in triplicate, and vancomycin and gentamicin were also tested in triplicate. Six untreated media controls were included on each plate. The plates were incubated at 35 °C for 18 h. The MIC was determined as the lowest concentration that inhibited visible growth of bacteria.

Eudistamide A (1)—White solid, $[\alpha]^{25}_D$ −51 (*c* 0.1, MeOH); UV (MeOH) λ (log ε) 209 (3.55), 224 (3.17), 280 (3.23); IR (ATR) ν_{max} 3300, 2953, 1648, 1535, 1519, 1450, 1320, 1242, 1072, 760, 677 cm^{-1}; ^1H and ^{13}C NMR (see Table S3; Supporting Information); HRMS $[M + H]^+$ *m/z* 1227.6882 (calcd for $C_{61}H_{91}N_{14}O_{13}$, 1227.6890).

Eudistamide B (2)—White solid, $[\alpha]^{25}_{D}$ + 37 (*c* 0.1, MeOH); UV (MeOH) λ (log ε) 207 (3.32), 223 (3.17), 279 (2.82); IR (ATR) ν_{max} 3290, 2932, 1738, 1647, 1532, 1517, 1455, 1314, 1244, 1072, 761, 669 cm^{-1}; ^{1}H and ^{13}C NMR (see Table S4; Supporting Information); HRMS $[M + H]^{+}$ *m/z* 1406.7253 (calcd for $C_{72}H_{100}N_{11}O_{18}$, 1406.7248).

Acid Hydrolysis of Eudistamides A (1) and B (2)—Separate solutions of compounds **1** and **2** (0.5 mg each) in 6 N HCl (1 mL) were hydrolyzed at 110 °C for 4 h and dried under vacuum.

Determination of Proteinogenic Amino Acid Configurations

L- and L/D-FDLA were synthesized as previously reported.[47] The hydrolysate was mixed with 1 N $NaHCO_3$ (40 μL), and 35 μL of L-FDLA (10 mg/mL in acetone). Each solution was stirred at 45 °C for 1 h, cooled to room temperature, quenched with 1 N HCl (40 μL), and dried under vacuum. Similarly, the standard L- and D-amino acid were derivatized separately. The derivatives of the hydrolysate of compound **1** and the standard amino acids were subjected to LC–MS analysis with a Phenomenex Kinetex C_{18} reversed-phase column (2.6 μm, 100 × 4.6 mm) at a flow rate of 0.5 mL/min and with a linear gradient of H_2O (containing 0.1% formic acid) and MeOH (90:10 to 0:100 over 15 min, and a hold at 100% MeOH for 5 min). The absolute configurations of the amino acids were determined by comparing the retention times of the L- and D-amino acids derivatives, which were identified by MS. The absolute configurations of the amino acids in **1** were assigned based on a comparison of retention time of amino acid standards derivatized with L-FDLA. In a similar manner, the derivatives of the hydrolysate of compound **2** and the standard amino acids were subjected to LC–MS analysis with a Phenomenex Luna C_{18} reversed-phase column (5.0 μm, 250 × 4.6 mm) at a flow rate of 1.0 mL/min and with a linear gradient of H_2O (containing 0.1% formic acid) and ACN (90:10 to 0:100 over 30 min, and a hold at 100% ACN for 5 min). The retention times and ESIMS data for L-FDLA derivatives of the hydrolysates and the standard amino acids are summarized in Tables S5 and S6 (Supporting Information).

Synthesis of (2*R*,3*S*)-3-Hydroxyleucine and (2*R*,3*R*)-3-Hydroxyleucine and Advanced Marfey's Analysis of 3-Hydroxyleucines

(2*R*,3*S*)-3-Hydroxyleucine and (2*R*,3*R*)-3-hydroxyleucine were synthesized using the procedures by Bonnard et al.[32] We obtained 20.0 mg of major precursor (*S*)-1-((2*R*,5*S*)-5-isopropyl-3,6-dimethoxy-2,5-dihydropyrazin-2-yl)-2-methylpropan-1-ol and 2.5 mg of minor precursor (*R*)-1-((2*R*,5*S*)-5-isopropyl-3,6-dimethoxy-2,5-dihydropyrazin-2-yl)-2-methylpropan-1-ol. The hydroxyleucine precursors were hydrolyzed following the general peptide acid hydrolysis process. The major precursor gave a mixture of (2*R*,3*S*)-3-hydroxyleucine and D-valine, and the minor precursor gave a mixture of (2*R*,3*R*)-3-hydroxyleucine and D-valine. These two hydrolysate mixtures were derivatized with L-FDLA and L/D-FDLA, respectively, resulting in four products: (2*R*, 3*S*)-3-hydroxyleucine-L-FDLA, (2*R*, 3*S*)-3-hydroxyleucine-D-FDLA, (2*R*, 3*R*)-3-hydroxyleucine-L-FDLA, and (2*R*, 3*R*)-3-hydroxyleucine-D-FDLA. Among these four products, (2*R*, 3*S*)-3-hydroxyleucine-D-FDLA will show the same retention time as (2*S*, 3*R*)-3-hydroxyleucine-L-FDLA, and (2*R*, 3*R*)-3-hydroxyleucine-D-FDLA will show the same retention time as (2*S*, 3*S*)-3-hydroxyleucine-L-FDLA, under the nonchiral HPLC condition we used in advanced Marfey's analysis. The

resulting four derivatization mixtures were subjected to LC–MS analysis with a Phenomenex Luna C_{18} reversed-phase column (5.0 μm, 250 × 4.6 mm) at a flow rate of 1.0 mL/min and with a linear gradient of H_2O (containing 0.1% formic acid) and ACN (25:75 to 65:35 over 50 min). When these four retention times were compared with the retention time of hydrolysate-L-FDLA derivative of compound **2**, the two 3-hydroxyleucines in the peptide were assigned as 2*S*, 3*R*. Detailed retention times of four isomers and hydrolysate could be found in Table S6 (Supporting Information). ^{1}H NMR data of (*S*)-1-((2*R*,5*S*)-5-isopropyl-3,6-dimethoxy-2,5-dihydropyrazin-2-yl)-2-methylpropan-1-ol ($CDCl_3$, 500 MHz): δ 4.09 (1H, m), 3.99 (1H, m), 3.73 (3H, s), 3.69 (3H, s), 3.63 (1H, br), 2.25 (1H, m), 2.01, (1H, m), 1.64 (1H, br), 1.04 (3H, d, *J* = 7.0 Hz), 1.03 (3H, d, *J* = 7.0 Hz), 0.99 (3H, d, *J* = 7.0 Hz), 0.71 (3H, d, *J* = 7.0 Hz). ^{1}H NMR data of (*R*)-1-((2*R*,5*S*)-5-isopropyl-3,6-dimethoxy-2,5-dihydropyrazin-2-yl)-2-methylpropan-1-ol ($CDCl_3$, 500 MHz): δ 4.10 (1H, t, *J* = 3.5 Hz), 3.92 (1H, t, *J* = 3.5 Hz), 3.65 (3H, s), 3.64 (3H, s), 3.59 (1H, br), 2.20 (1H, m), 1.76, (1H, m), 1.51 (1H, br), 0.98 (3H, d, *J* = 7.0 Hz), 0.85 (3H, d, *J* = 7.0 Hz), 0.84 (3H, d, *J* = 7.0 Hz), 0.63 (3H, d, *J* = 6.9 Hz).

Organisms, Media, and Antibiotic of in Vivo Studies

Eudistamide B (**2**) was tested for antibacterial activity in vivo studies. One isolate of *E. coli* ATCC 25922 and *S. aureus* ATCC 25923, separeatly, was used for these studies. Organisms were grown, subcultured, and quantified using Mueller-Hinton broth (MHB) and agar (Difco Laboratories, Detroit, MI).

Animals

Six week-old, specific pathogen-free, female ICR/Swiss mice weighing 24–27 g were used for all studies (Harlan Sprague–Dawley, Indianapolis, IN). Animals were maintained in accordance with the American Association for Accreditation of Laboratory Animal Care (AAALAC) criteria. All animal studies were approved by the Animal Research Committees of the William S. Middleton Memorial VA Hospital and the University of Wisconsin.

Murine Thigh Infection Model

Mice were rendered neutropenic (neutrophils <100/mm^3) by injecting cyclophosphamide (Mead Johnson Pharmaceuticals, Evansville, IN) intraperitoneally 4 days (150 mg/kg) and 1 day (100 mg/kg) before thigh infection. Previous studies have shown that this regimen produces neutropenia in this model for 5 days. Broth cultures of freshly plated bacteria were grown to logarithmic phase overnight to an absorbance of 0.3 at 580 nm (Spectronic 88; Bausch and Lomb, Rochester, NY). After a 1:10 dilution into fresh MHB, bacterial counts of the inoculum ranged from 106.3 to 6.9 cfu/mL. Thigh infections with each of the isolates were produced by injection of 0.1 mL of inoculum into the thighs of isoflorane-anesthetized mice 2 h before therapy.

In Vivo Time Kill and PAE

Two hours after thigh infection with either single doses of compound **2** (4, 8, 16, 32, and 64 mg/kg) by the intraperitoneal or intravenous route, groups of two treated and untreated mice were sacrificed at each treatment end point (0 h at the start of therapy and 6 h after

treatment). The thighs (four per treatment group) were immediately removed upon euthanasia and processed for cfu determination. The burden of organisms in the thigh was measured by viable plate counts of tissue homogenates. The impact of each dose on the burden of organisms was measure over time of the study period.

Supplementary Material

Refer to Web version on PubMed Central for supplementary material.

ACKNOWLEDGMENTS

This work was supported by funding from the University of Wisconsin—Madison School of Pharmacy. This work was also funded in part by the U19 AI109673, NIH, and NIGMS Grant R01 GM107557. We thank the Analytical Instrumentation Center (AIC) at the University of Wisconsin—Madison School of Pharmacy for the facilities to acquire spectroscopic data, especially MS data. This study made use of the National Magnetic Resonance Facility at Madison (NMRFAM), which is supported by NIH grants P41RR02301 (BRTP/NCRR) and P41GM66326 (NIGMS).

REFERENCES

1. Livermore DM. Clin. Microbiol. Infect. 2004; 10:1–9. [PubMed: 15522034]
2. a Lautru S, Deeth RJ, Bailey LM, Challis GL. Nat. Chem. Biol. 2005; 1:265–269. [PubMed: 16408055] b Bentley SD, et al. Nature. 2002; 417:141–147. [PubMed: 12000953]
3. Doroghazi JR, Albright JC, Goering AW, Ju K, Haines RR, Tchalukov KA, Labeda DP, Kelleher NL, Metcalf WM. Nat. Chem. Biol. 2014; 10:963–968. [PubMed: 25262415]
4. Forner D, Berrué F, Correa H, Duncan K, Kerr RG. Anal. Chim. Acta. 2013; 805:70–79. [PubMed: 24296145]
5. Gill KA, Berrué F, Arens JC, Kerr RG. J. Nat. Prod. 2014; 77:1372–1376. [PubMed: 24927492]
6. Hoffmann T, Krug D, Hüttel S, Müller R. Anal. Chem. 2014; 86:10780–10788. [PubMed: 25280058]
7. Nguyen DD, Wu C, Moree WJ, Lamsa AL, Medema MH, Zhao X, Gavilan RG, Aparicio M, Atencio L, Jackson C, Ballesteros J, Sanchez J, Watrous JD, Phelan VV, van de Wiel C, Kersten RD, Mehnaz S, Mot RD, Shank EA, Charusanti P, Nagarajan H, Duggan BM, Moore BS, Bandeira N, Palsson BØ, Pogliano K, Gutiérrez M, Dorrestein PC. Proc. Natl. Acad. Sci. U. S. A. 2013; 110:E2611–E2620. [PubMed: 23798442]
8. Hou Y, Braun DR, Michel CR, Klassen JL, Adnani N, Wyche TP, Bugni TS. Anal. Chem. 2012; 84:4277–4283. [PubMed: 22519562]
9. Wyche TP, Hou Y, Vazquez-Rivera E, Braun D, Bugni TS. J. Nat. Prod. 2012; 75:735–740. [PubMed: 22482367]
10. Hou Y, Tianero DB, Kwan JC, Wyche TP, Michel CR, Ellis GA, Vazquez-Rivera E, Braun DR, Rose WE, Schmidt EW, Bugni TS. Org. Lett. 2012; 14:5050–5053. [PubMed: 22984777]
11. Wyche TP, Piotrowski JS, Hou Y, Braun D, Deshpande R, McIlwain S, Ong IM, Myers CL, Guzei IA, Westler WM, Andes DR, Bugni TS. Angew. Chem., Int. Ed. 2014; 53:11583–11586.
12. Samat N, Tan PJ, Shaari K, Abas F, Lee HB. Anal. Chem. 2014; 86:1324–1331. [PubMed: 24405504]
13. a Kikuchi Y. Microbes Environ. 2009; 24:195–204. [PubMed: 21566374] b Poulsen M, Oh D, Clardy J, Currie CR. PLoS One. 2011; 6:e16763. [PubMed: 21364940]
14. a Sogin ML, Morrison HG, Huber JA, Welch DM, Huse SM, Neal PR, Arrieta JM, Herndl GJ. Proc. Natl. Acad. Sci. U. S. A. 2006; 103:12115–12120. [PubMed: 16880384] b Andrianasolo EH, Haramaty L, Rosario-Passapera R, Bidle K, White E, Vetriani C, Falkowski P, Lutz R. J. Nat. Prod. 2009; 72:1216–1219. [PubMed: 19507867]

15. a Schabereiter-Gurtner C, Saiz-Jimenez C, Pinar G, Lubitz W, Rölleke S. FEMS Microbiol. Ecol. 2003; 1606:1–13.b Engel AS, Porter ML, Stern LA, Quinlan S, Bennett PC. FEMS Microbiol. Ecol. 2004; 51:31–53. [PubMed: 16329854]
16. a Wang X, Shaaban KA, Elshahawi SI, Ponomareva LV, Sunkara M, Zhang Y, Copley GC, Hower JC, Morris AJ, Kharel MK, Thorson JS. J. Nat. Prod. 2013; 76:1441–1447. [PubMed: 23944931] b Shaaban KA, Wang X, Elshahawi SI, Ponomareva LV, Sunkara M, Copley GC, Hower JC, Morris AJ, Kharel MK, Thorson JS. J. Nat. Prod. 2013; 76:1619–1626. [PubMed: 23947794]
17. a Lam KS. Curr. Opin. Microbiol. 2006; 9:245–251. [PubMed: 16675289] b Abdelmohsen UR, Bayer K, Hentschel U. Nat. Prod. Rep. 2014; 31:381–399. [PubMed: 24496105]
18. Reibarkh M, Wyche TP, Bugni TS, Martin GE, Williamson RT. Structure elucidation of uniformly ^{13}C labeled small molecule natural products. Magn. Reson. Chem. 2015 in press.
19. Ellis GA, Wyche TP, Fry CG, Braun DR, Bugni TS. Mar. Drugs. 2014; 12:1013–1022. [PubMed: 24534844]
20. a Fellermeier M, Eisenreich W, Bacher A, Zenk MH. Eur. J. Biochem. 2001; 268:1596–1604. [PubMed: 11248677] b Watanabe H, Tetsuo T, Oikawa H. Tetrahedron Lett. 2006; 47:1399–1402.c Kwon Y, Park S, Shin J. Arch. Pharmacal Res. 2014; 37:967–971.
21. Kay LE, Ikura M, Tschudin R, Bax AJ. Magn. Reson. 1990; 89:496–514.
22. Clubb RT, Thanabal V, Wagner GJ. Magn. Reson. 1992; 97:213–217.
23. Grzesiek S, Bax AJ. Magn. Reson. 1992; 99:201–207.
24. Grzesiek S, Bax AJ. Am. Chem. Soc. 1992; 114:6291–6293.
25. Bax A, Ikura MJ. Biomol. NMR. 1991; 1:99–104.
26. Grzesiek S, Anglister J, Bax AJ. Magn. Reson., Ser. B. 1993; 101:114–119.
27. Grzesiek SJ, Bax AJ. Biomol. NMR. 1993; 3:185–204.
28. Bottomley MJ, Macias MJ, Liu Z, Sattler MJ. Biomol. NMR. 1999; 13:381–385.
29. Bax A, Clore M, Gronenborn AM. J. Magn. Reson. 1990; 88:425–431.
30. Siemion IZ, Wieland T, Pook KH. Angew. Chem., Int. Ed. Engl. 1975; 14:702–703. [PubMed: 812384]
31. a Harada K, Fujii K, Mayumi T, Hibino Y, Suzuki M. Tetrahedron Lett. 1995; 36:1515–1518.b Harada K, Fujii K, Hayashi K, Suzuki MM. Tetrahedron Lett. 1996; 37:3001–3004.c Fujii K, Ikai Y, Oka H, Suzuki M, Harada K. Anal. Chem. 1997; 69:5146–5151.
32. Bonnard I, Rolland M, Salmon J, Debiton E, Bartheomeuf C, Banaigs BJ. Med. Chem. 2007; 50:1266–1279.
33. a Hayashi K, Hashimoto M, Shigematsu N, Nishikawa M, Ezaki M, Yamashita M, Kiyoto S, Okuhara M, Kohsaka M, Imanaka H. J. Antibiot. 1992; 45:1055–1063. [PubMed: 1381343] b Yu Z, Vodanovic-Jankovic S, Kron M, Shen B. Org. Lett. 2012; 14:4946–4949. [PubMed: 22967068]
34. Shiomi K, Yang H, Inokoshi J, Van der Pyl D, Nakagawa A, Takeshima H, Omura S. J. Antibiot. 1993; 46:229–234. [PubMed: 8468236]
35. Bae M, Kim H, Moon K, Nam S, Shin J, Oh K, Oh D. Org. Lett. 2015; 17:712–715. [PubMed: 25622093]
36. Toki S, Agatsuma T, Ochiai K, Saitoh Y, Ando K, Nakanishi S, Lokker NA, Giese N, Matsuda YJ. Antibiot. 2001; 54:405–414.
37. Pohle S, Appelt C, Roux M, Fieldler H, Süssmuth RD. J. Am. Chem. Soc. 2011; 133:6194–6205. [PubMed: 21456593]
38. Um S, Park SH, Kim J, Park HJ, Ko K, Bang H, Lee SK, Shin J, Oh D. Org. Lett. 2015; 17:1272–1275. [PubMed: 25686280]
39. a Wohlleben W, Stegmann E, Süssmuth RD. Methods Enzymol. 2009; 458:459–486. [PubMed: 19374994] b Gunasekera SP, Ritson-Williams R, Paul VJ. J. Nat. Prod. 2008; 71:2060–2063. [PubMed: 19007282] c Cai G, Napolitano JG, McAlpine JB, Wang Y, Jaki BU, Suh J, Yang SH, Lee I, Franzblau SG, Pauli GF, Cho S. J. Nat. Prod. 2013; 76:2009–2018. [PubMed: 24224794] d Hou Y, Tianero DB, Kwan JC, Wyche TP, Michel CR, Ellis GA, Vazquez-Rivera E, Braun DR, Rose WE, Schmidt EW, Bugni TS. Org. Lett. 2012; 14:5050–5053. [PubMed: 22984777]
40. O'Sullivan J, McCullough JE, Tymiak AA, Kirsch DR, Trejo WH, Principe PA. J. Antibiot. 1988; 41:1740–1744. [PubMed: 3209465]

41. a Salzmann M, Pervushin K, Wider G, Senn H, Wüthrich K. J. Am. Chem. Soc. 2000; 122:7543–7548.b Liang B, Tamm LK. Proc. Natl. Acad. Sci. U. S. A. 2007; 104:16140–16145. [PubMed: 17911261] c Sakakibara D, Sasaki A, Ikeya T, Hamatsu J, Hanashima T, Mishima M, Yoshimasu M, Hayashi N, Mikawa T, Wälchli M, Smith BO, Shirakawa M, Güntert P, Ito Y. Nature. 2009; 458:102–106. [PubMed: 19262674]
42. Van Name WGZ. Kristallogr. - Cryst. Mater. 1902; 11:325–412.
43. Harrison PJ, Waters RE, Taylor FJR. J. Phycol. 1980; 16:28–35.
44. Reasoner DJ, Geldreich EE. Appl. Environ. Microbiol. 1985; 49:1–7. [PubMed: 3883894]
45. Maldonado LA, Fragoso-Yañez D, Pérez-García A, Rosellón-Druker J, Quintana ET. Antonie van Leeuwenhoek. 2009; 95:111–120. [PubMed: 19023674]
46. National Committee for Clinical Laboratory Standards. Methods for Dilution Antimicrobial Susceptibility Tests for Bacteria that Grow Aerobically. 7th ed.. NCCLS; Villanova, PA: 2006. p. M7-A7.Approved standard
47. Marfey P. Carlsberg Res. Commun. 1984; 49:591–596.

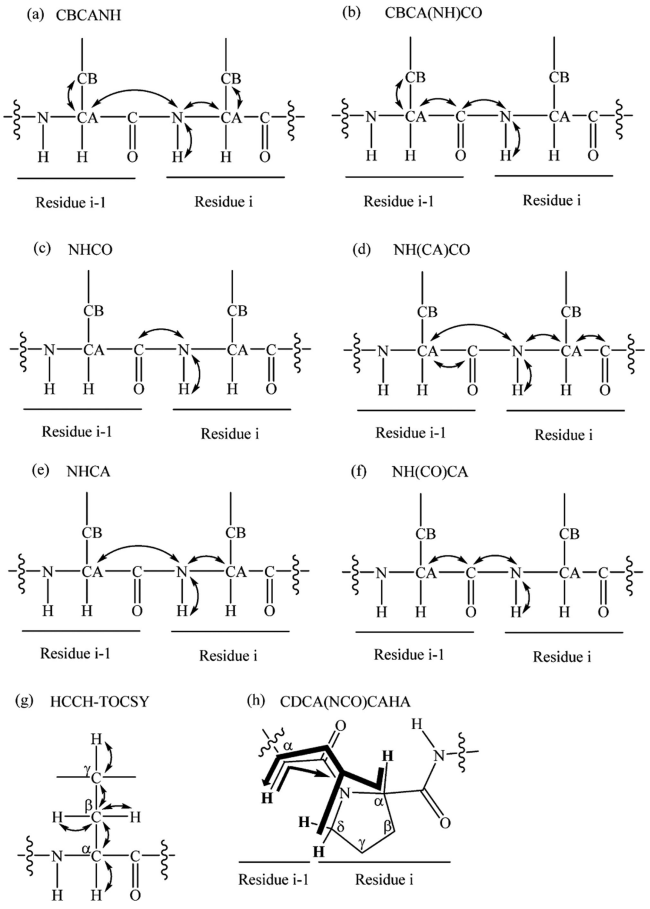

Figure 1.

Connectives observed in seven different types of 3D NMR experiment. (a) The CBCANH experiment correlates the chemical shift of amide resonance with the C_{α} and C_{β} of both inter- and intraresidue. (b) The CBCA(CO)NH experiment only correlates the amide resonance with C_{α} and C_{β} of the preceding residue. (c) The NHCO experiment provides the connectives between the amide of a residue (NH_i) with the carbonyl carbon of the preceding residue (CO_{i-1}). (d) The NH(CA)CO experiment shows the amide resonance (NH_i) is correlated with the carbonyl carbon of the same residue (CO_i), as well as that of the preceding residue (CO_{i-1}). (e) The NHCA experiment correlates the amide resonance (NH_i) with the C_{α} of the same residue and preceding residue. (f) The NH(CO)CA experiment only correlates the resonances of the amide with the C_{α} of the preceding residue. (g) The HCCH-TOCSY correlates a $^{1}H/^{13}C$ pair to all other protons in the same aliphatic side chain. (h) The thick arrow represents pathways utilizing the ^{1}J ($C^{\alpha/\delta}$, N) coupling, whereas the thin arrow represents the less efficient pathway via ^{2}J (C^{α}, N). Protons directly involved in the transfer pathways are shown in bold font.

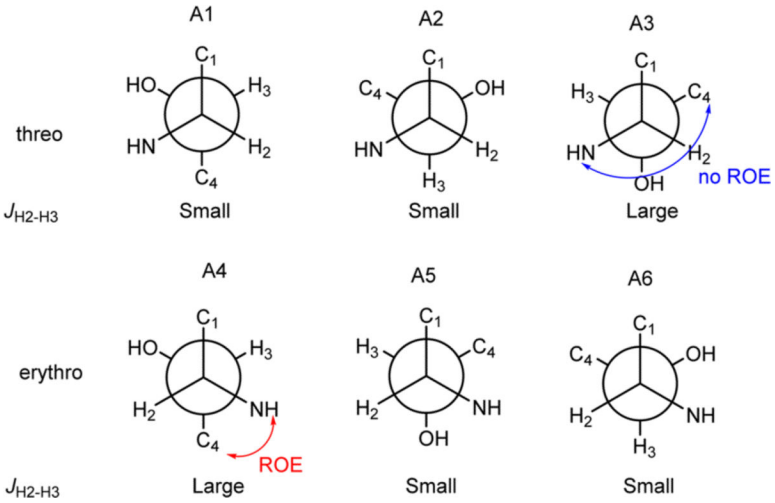

Figure 2.

J-based configuration analysis of C-2 and C-3 of compound **2**.

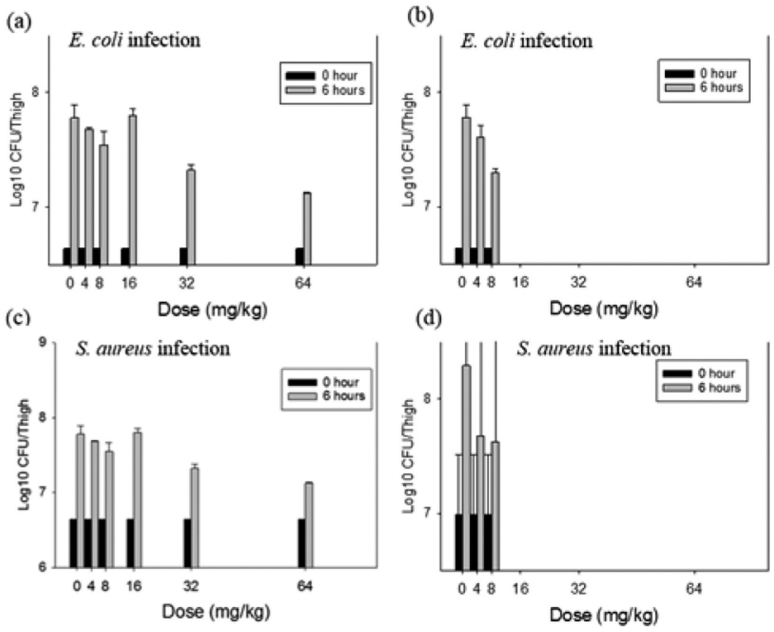

Figure 3.

In vivo time kill experiment with compound **2** using a neutropenic mouse thigh model. Each symbol represents the mean and standard deviation from four thighs of two mice infected with either *E. coli* or *S. aureus*. The error bars represent the standard deviation. Five single doses (4, 8, 16, 32, and 64 mg/kg) of compound **2** were administered to mice. (a) *E. coli* infected murine thighs treated with five single doses of **2** by intraperitoneal route. (b) *E. coli* infected murine thighs treated with five single doses of **2** by intravenous route. (c) *S. aureus* infected murine thighs treated with five single doses of **2** by intraperitoneal route. (d) *S. aureus* infected murine thighs treated with five single doses of **2** by intravenous route. The (b) and (d) regimens do not include the 16, 32, and 64 mg/kg since the mice died following administration.